Int. J. Electrochem. Sci., 12 **(2017)** 1992 – 2002, doi: 10.20964/2017.03.50

International Journal of
ELECTROCHEMICAL
SCIENCE
www.electrochemsci.org

Mechanism and Effectiveness of Ti-based Nano-Electrode for Electrochemical Denitrification

Lele Wang[1,2], *Miao Li*[2,*], *Xiang Liu*[2,*], *Chuanping Feng*[1], *Fang Zhou*[2], *Nan Chen*[1], *Weiwu Hu*[1]

[1] School of Water Resources and Environment, China University of Geosciences (Beijing), Beijing 100083, China
[2] School of environment, Tsinghua University, Beijing 100084, China
[*]E-mail: watersml@126.com, x.liu@tsinghua.edu.cn

Received: 2 September 2016 / *Accepted:* 12 January 2017 / *Published:* 12 February 2017

A novel Ti-based nano-electrode was fabricated to improve electrochemical nitrate reduction efficiency. The results of scanning electron microscopy (SEM) and X-ray photoelectron spectroscopy (XPS) demonstrated that the surface of the Ti-based nano-electrode was covered with a large number of nanoparticles, as well as relatively homogenous tubular structure, and that the main component of the electrode was TiO_2. Cyclic voltammetry (CV) analysis of Ti-based nano electrode result indicated that it was capable of enhanced electrochemical activity in comparison with Ti electrode. It was found that nitrate was removed efficiently by electrochemical means using the Ti-based nano-electrode as cathode with a Ti/Pt anode. The developed system was able to promote the electrochemical reduction of nitrate under a range of experimental conditions. The addition of NaCl was found to positively affect the removal of by-products, and thus, in combination with nitrate reduction, achieved the goal of clean, safe removal of pollutants.

Keywords: Ti-based nano-electrode, Nitrate, Reduction efficiency, Electrochemical approach

1. INTRODUCTION

Nitrate contamination of water resources has become an increasingly serious environmental problem [1]. Nitrate contamination water above the permissible limit for drinking water is also hazardous to human health, including “blue baby syndrome,” methemoglobinemia and cancer [2, 3]. The main sources of nitrate are overfertilization, animal feces, industrial effluents and human wastes [4, 5]. The World Health Organization (WHO) and the United States Environmental Protection Agency (USEPA) permit a maximum limit of 50 mg/L for nitrate in drinking water [6, 7]. Among nitrate removal methods, biological denitrification requires extensive monitoring including pH control, temperature maintenance and the addition of carbon sources [8], while both reverse osmosis and ion

exchange [9, 10] produce large amounts of nitrate, resulting in secondary pollution and requiring further treatment. In contrast, the electrochemical reduction of nitrate has recently attracted a great deal of attention because of its high treatment efficiency, environmental sustainability and low investment cost [11]. The cathodic reduction of nitrate has been widely investigated by using various electrode materials (such as Cu, Fe, Ti, Cu/Zn, Ni, Pb and Pt) [12-17]. Among these materials, Cu and Fe as relatively efficient promoters are usually used for nitrate electroreduction [14, 17]. A Pd–Cu cathode was shown to have a very high selectivity towards the electroreduction of nitrate to N_2 when the Pd/Cu surface ratio and the electrode potential were accurately controlled, but the efficiency was very low [18]. The mechanism for the electrolytic reduction of nitrate is complex and the electrochemical reduction of nitrate also may produce a large number of products (NH_2OH, N_2O and NH_3)[19, 20]. Hence, it is crucial to produce an appropriate cathode material to increase the reduction efficiency of nitrate.

Recently, novel TiO_2 nanotubes [21], with large specific surface area, pore volume and high surface energy, have been widely used in water splitting, self-cleaning materials dye-sensitized cells, photocatalysis and biocompatible materials [22-27]. TiO_2 nanotubes with optical and electrochemical properties often exhibit unique electrochemical performance in the degradation of organic compounds in wastewater and the generation of hydrogen via water splitting [22, 27]. As far as we know, the use of nano-electrodes for the electrochemical reduction of nitrate has seldom been reported previously. In our previous study [28], we fabricated a novel Ti-based nano-cathode for electrochemical denitrification using a Box-Behnken design. However, the mechanism and effectiveness of the Ti-based nano-electrode were not investigated. Liu et al., [29, 30] fabricated a novel Cu/Ti bilayer nanoelectrode and Cu-Zn/TiO_2 nanotube array polymetallic nanoelectrode for electroreduction nitrate achieving a high removal eficiency.

Nanometer-scale electrodes, with high specific surface areas, often exhibit distinctive electrochemical properties compared with other materials. The enlarged surface of a nanometer-scale electrode with a double-layer structure was shown to increase the electronic diffusion velocity and charge-carrier lifetime, leading to an enhanced electrochemical capability [31]. It thereby exhibited an excellent electrochemical activity for the removal of pollutants, with high efficiency. In this study, we produced a novel Ti-based nano-cathode for electrochemical denitrification. The mechanism of the Ti-based nano-electrode was studied by electrochemical investigation of its morphology, crystal structure and electrochemical performance. The effects of several parameters, including current density, initial nitrate concentration, temperature and quantity of NaCl addition, were studied. The aim of this work was to produce a highly efficient Ti-based nano-cathode and investigate the mechanism and performance of the cathode for the reduction of nitrate in an undivided cell.

2. MATERIALS AND METHODS

2.1 Preparation of Ti-based nano electrodes

The fabrication process of the nano-electrode was similar to that of the previous study [28]. TiO_2 nanotube arrays were prepared on Ti electrode (0.02mm, 99.6% purity). The samples were

polished with sandpaper before electrochemical anodization, rinsed in deionized water and dried in air. About 100 mL solution which contains acetic acid (acetic acid and deionized water mixed in a 1:10 volume ratio) and 0.05 wt% HF were poured in an electrolysis cell. The cleaned titanium foil used as the cathode and a graphite electrode as the anode. Then the voltage was set to 25 V and the experiment lasted for 2 h. The anodization process was performed at room temperature. After the anodization, samples were cleaned with ultrasonically in deionized water, then used after dried.

2.2 Electrochemical measurements

Cyclic voltammetric (CV) measurements were performed with an electrochemical workstation (CHI 660D, Shanghai Chenhua instruments, China) at room temperature with the Ti and Ti-based nano electrode as a working electrodes, Pt electrode as a counter electrode and Ag/AgCl (sat.) electrode as the reference electrode. All quoted potentials are relative to the Ag/AgCl (sat.) reference electrode. Solutions were prepared with reagent grade chemicals and ultra-pure water (resistivity–18.2MΩ·cm). The working electrode was cycled from −1.4 V to +0.2 V at a scan rate of 100mV/s three times before collecting stable polarization data.

2.3 Batch electrolysis

For electrolysis experiments, the Ti-based nano-electrode was used as the cathode and a Ti/Pt electrode (Toho Technology, Japan) used as anode. The electrode area is 25 cm^2 and the distance between the electrodes was 8 mm. Approximately 100 mL of synthetic nitrate solution (50 mg/L) was poured into the electrochemical cell; 0.5 g/L Na_2SO_4 was also added into all the experiments to enhance the conductivity. The reaction was carried out with the application of a specified current density controlled by a direct-current power supply (HY1792-5S，Guodianyaguang，China).

To investigate the effect of the current density, it was set at five different values, i.e., 12, 25, 37, 50 and 62 mA/cm^2, under galvanostatic control. The effect of the initial nitrate concentration was investigated at 20, 30, 50, 70 and 100 mg/L. To study the effect of temperature, the experiments were performed at 0^oC, 20^oC, 40^oC and 60^oC, maintained by a water bath. NaCl was added into the synthetic nitrate solution at concentrations of 0, 0.5 and 1.0 g/L to investigate the effect of the NaCl dosage.

2.4 Analysis

At different intervals 1.5 mL of sample was taken from the electrochemical cell for analysis and the electrolysis was ceased after 90 min. Nitrate was detected by standard colorimetric method using spectrophotometer (752N, China). Nitrite was colorimetrically analyzed by N-(1-naphthyl)-ethylenediamine spectrophotometry. Ammonia was measured by Nesslerization reagent spectrophotometer [32]. Surface morphology of electrodes was observed by ultra-high resolution scanning electron microscope (Hitachi S5500, Japan). The element of the sample and chemical composition were characterized by X-ray photoelectron spectrometer (Escalab 250XI, USA).

3. RESULTS AND DISCUSSION

3.1 Electrode characterization and electrochemical denitrification mechanism

Scanning electron microscopy (SEM) images of the Ti electrode and Ti-based nano-electrode are shown in Figure 1. The surface morphology of the Ti was characterized by a rough and irregular shape, with no growth of nanotubular layers (Fig. 1a).

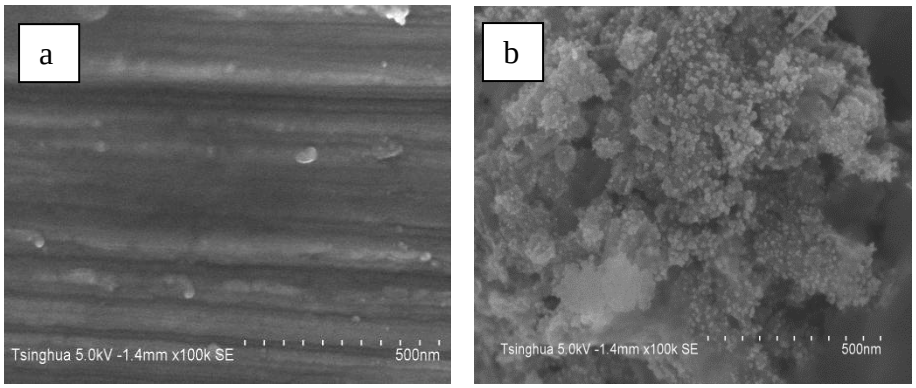

Figure 1. Scanning electron microscopy images of (a) Ti electrode and (b) Ti-based nano-electrode.

The surface of the Ti-based nano electrode was covered with a large number of nanoparticles, compressed into a sponge, and it also contained with relatively homogenous tubular structure (Fig. 1b). The composition of the electrode was determined by energy-dispersive spectroscopy (EDS), as shown in Fig. 2. It can be seen that the Ti electrode contained100 wt% Ti (Fig. 2a), while the Ti-based nano electrode contained 62.41 wt% Ti and 37.59 wt% O (Fig. 2b). It could be inferred that the Ti-based nano-electrode mainly existed in the form of a compound of Ti and O; however, the specific nature of the material required further verification.

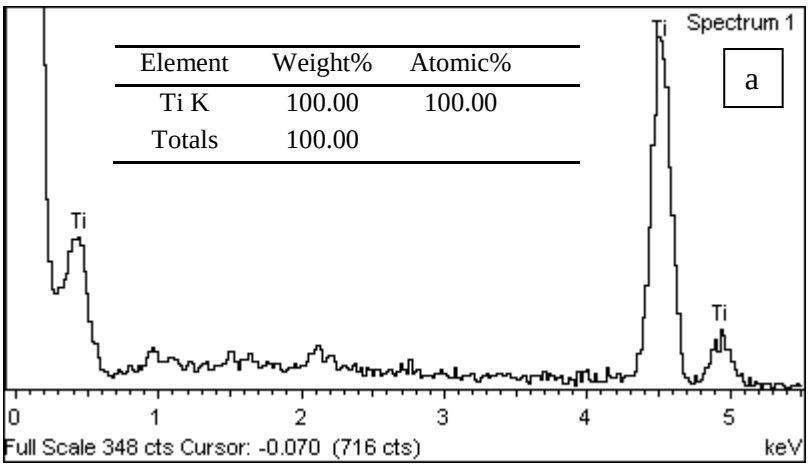

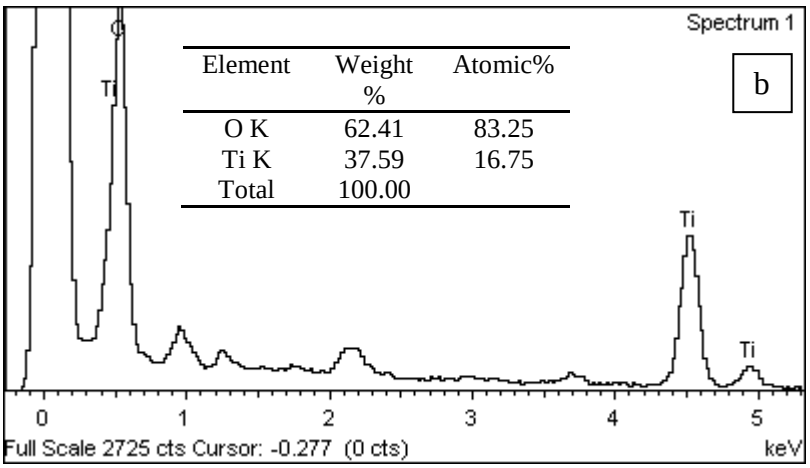

Figure 2. Energy dispersive spectrum of (a) Ti and (b) Ti-based nano-electrode

The surface oxidation states of the electrodes were determined by X-ray photoelectron spectroscopy (XPS). As can be seen in Fig. 3 (a), the Ti2p spectrogram contains two characteristic peaks at 458.5 and 464.3 eV, respectively, which correspond closely with the $Ti2p_{3/2}$ and $Ti2p_{1/2}$ electron binding energies, respectively. Moreover, the difference in electron binding energy between the two peaks is 5.8 eV, providing important evidence of Ti^{4+} in pure TiO_2 [33, 34]. From Fig. 3 (b), it can be seen that in the XPS spectrum, oxygen presents a broad, asymmetric peak, which shows that the oxygen on the surface of the nanotube array did not consist of a single species. The O1s scanning spectrum could be fitted to two peaks, at approximately 530.0 and 531.5 eV. These two values agree well with those found by Li et al. [35] for the binding energy of lattice oxygen and hydroxyl oxygen, respectively. This suggests that the nanotube array fabricated by the oxidation method used herein mostly consisted of these two chemical states. By comparing the peak areas, i.e., the left-hand peak was wider than the right, we concluded that O1s was mostly present in the form of lattice oxygen (Ti-O-Ti). This result is in accordance with the findings of EDS. Therefore, the nanotube arrays prepared by anodic oxidation in this study were mainly composed of TiO_2.

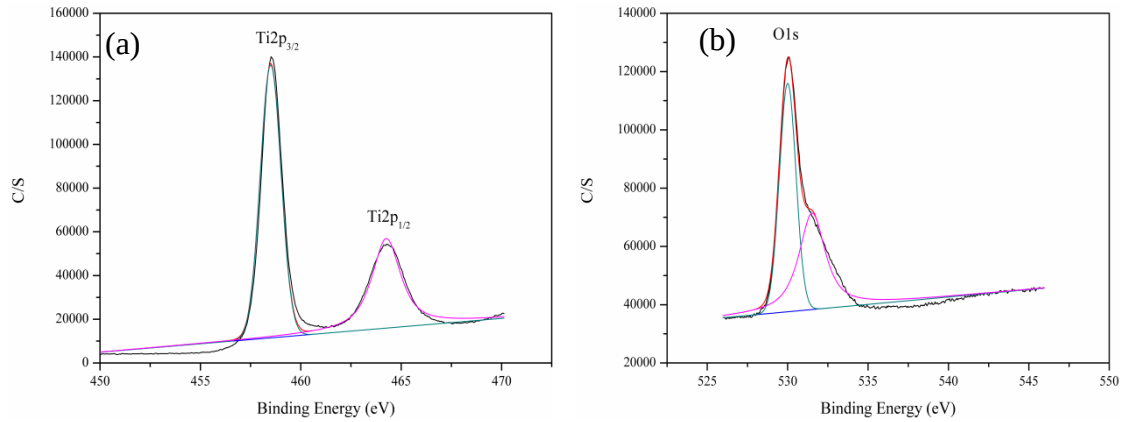

Figure 3. XPS spectra of Ti-based nano-electrode (a) Ti2p, (b) O1s

In this study, the Ti-based nano-electrode was prepared by anodic oxidation. The main reactions in this method are as follows [36, 37]:

$Ti + 2H_2O \rightarrow TiO_2 + 4H^+ + 4e$ (10)

$TiO_2 + 4H^+ + 6F^- \rightarrow [TiF_6]^{2-} + 2H_2O$ (11)

With the onset of anodization, a dense oxide was formed on the surface of the Ti electrode, after which a thin and compact TiO_2 layer was formed. In the presence of F^-, the oxide layer partially dissolved, forming pits (reaction (11)). Then, TiO_2 was corroded under the action of F^-, which consumed H^+, promoting the occurrence of reaction (10). The initial TiO_2 layer was thus formed in two steps. This two-step reaction occurred in a cycle, finally forming TiO_2 nanotubes with a range of the pore morphology.

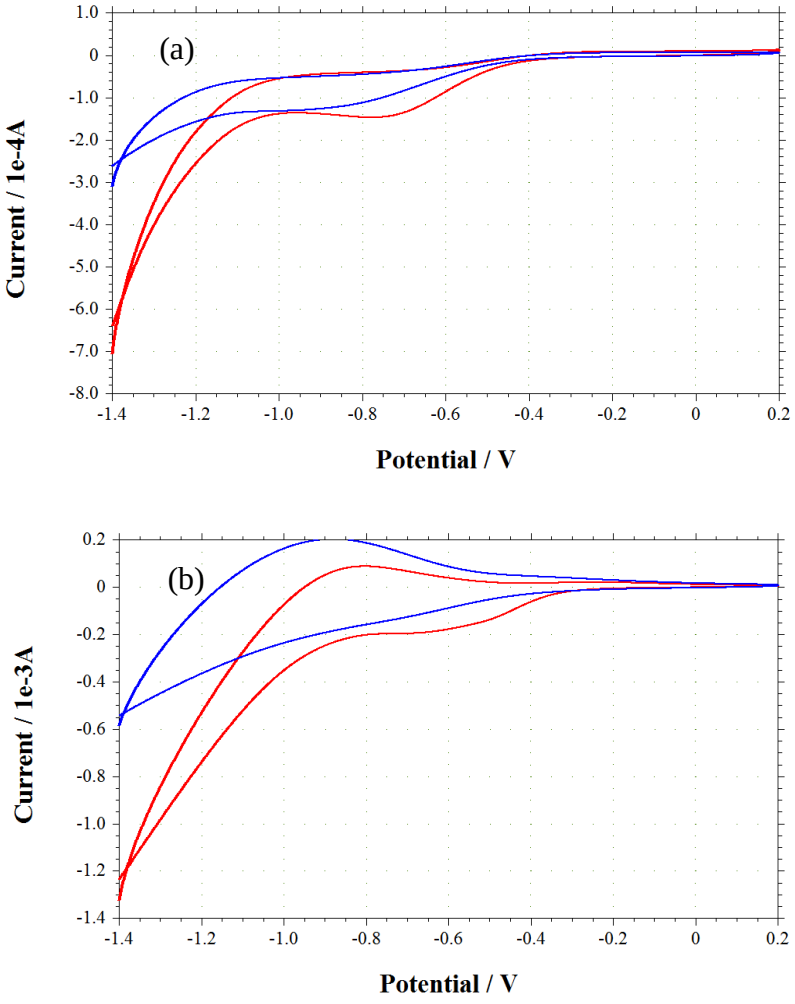

Figure 4. Cyclic voltammograms recorded at (a) Ti and (b) Ti-based nano-electrode in: (--) 0.50 g/L Na_2SO_4; (--) 0.50 g/L Na_2SO_4 +200 mg/L NO_3^--N.

Fig. 4 shows the cyclic voltammograms obtained for the reduction of nitrate at Ti and Ti-based nano-electrode. In the sodium sulfate electrolyte, the main process observed was water electrolysis to produce hydrogen at approximately −1.0 to −1.4 V. Throughout the process, the Ti-based nano-

electrode had a larger current fluctuation range than the Ti electrode and also showed stronger electrochemical activity. In Figure 4, clear peak can be observed at approximately E=−0.7 V (Fig. 4(a)) and E=−0.6 V (Fig. 4(b)). These peaks were attributed to the oxidation/reduction of NO_3^- ions converted to NO_2^-. This hypothesis has also been verified in electrolytic batch experiments. At electrolysis voltages of −0.70 and −0.60 V, the product of electrochemical reduction was NO_2^-, which conformed that NO_3^- ions were mostly converted to NO_2^- in this experiment.

3.2 Effect of electroreduction parameters

3.2.1 Effect of current density

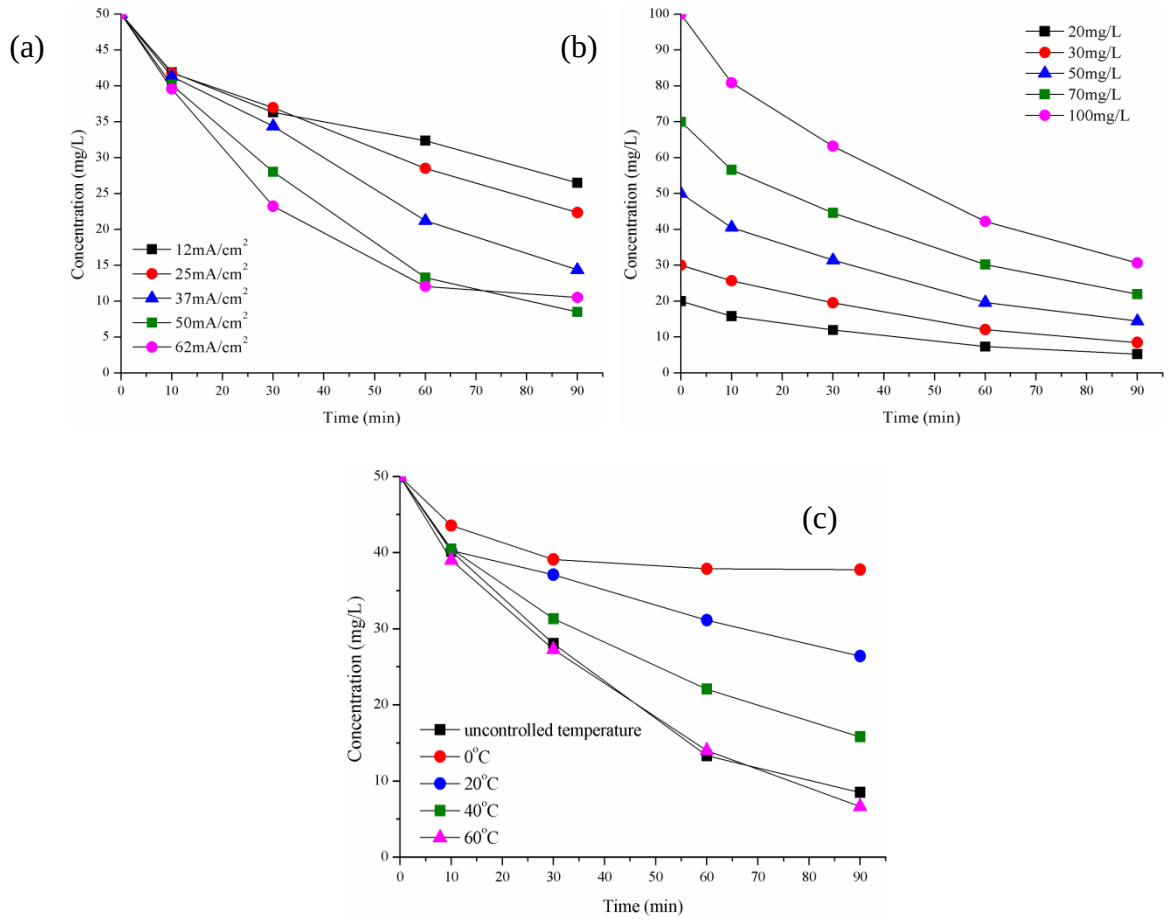

Figure 5. Electroreduction of nitrate at different (a) current densities, (b) initial nitrate concentrations, (c) temperatures, 0.50 g/L Na_2SO_4

Fig.5 (a) shows the reduction of nitrate at different current densities. As is shown, the concentration of nitrate decreased from 50 mg/L to 26.5, 22.4, 14.4, 8.5 and 10.5 mg/L in 90 min at 12, 25, 37, 50 and 62 mA/cm^2, respectively. The nitrate reduction rate increased with increasing current density in the range 12–50 mA/cm^2. This is probably because at increased current density, the cathode provides more electrons, which is advantageous to the reduction of nitrate. When the current density was increased from 50 to 62 mA/cm^2, the extent of nitrate reduction showed very little increase after

60 min electrolysis. This was probably because of the large amount of hydrogen gas generated at the surface of the electrode, which has an inhibitory effect on nitrate reduction. These results were consistent with studies by Li et al. [38], who found that using a Cu/Zn alloy and Ti/IrO_2-Pt as cathode and anode, respectively, the rate of nitrate reduction increased only slightly as the current density increased from 10 to 60 mA/cm^2. At a current density of 12, 25, 37, 50 and 62 mA/cm^2, the potentials were in the ranges of 8.4–9.9, 11.5–16.1, 12.7–21.4, 14.7–28.9 and 16.4–31.9 V, respectively. At current densities of 50 mA/cm^2, the nitrate reduction efficiency was 286.2% higher than that from the untreated electrode (which reduced the concentration of nitrate from 50.0 to 40.6 mg/L). To maximize the trade-off between nitrate treatment efficiency and economic considerations, a lower current density is favorable. The results of this study suggest that 50 mA/cm^2 may be the optimum current density.

3.2.2 Effect of initial nitrate concentration

The variation of the nitrate concentration during constant-current electrolysis in the electrolytic cell with different initial nitrate concentrations is reported in Fig. 5(b). As is shown, the trends of electrochemical reduction of nitrate were similar under different initial nitrate concentrations. With increasing initial concentration, the removal efficiency decreased. The removal efficiencies were 73.5%, 71.7%, 70.9%, 68.7% and 69.4% for 20, 30, 50, 70 and 100 mg/L nitrate solutions, respectively. This is consistent with the notion that a high concentration inhibits the mass transfer of nitrate to the electrode and thus impedes the reduction of nitrate.

3.2.3 Effect of temperature

Fig. 5(c) shows the effect of reaction temperature on nitrate reduction. The previous experiments were performed at a constant temperature of 25 °C. We can see that the nitrate removal efficiency increased with increasing temperature. This can be explained by the fact that increasing the temperature increases both the rate of diffusion and the strength of adsorption of nitrate, which facilitates its reduction [39]. The nitrate removal efficiency at uncontrolled temperature was similar to that at 60 °C. In the sample without temperature control, the temperature of the treated solution increased from 25 °C to 80 °C after 90 min electrolysis.

3.2.4 Effect of different NaCl dosage

Fig. 6 shows the variation of nitrate-N, ammonia-N and nitrite-N during electrolysis under different concentrations of NaCl. It can be seen that the electrochemical of nitrate proceeded differently with different dosages of NaCl, and the formation of by-products also varied. When there is no NaCl in the system (Fig. 6 (a)), the concentration of nitrate decreased from 50 to 11.6 mg/L in 90 min. That of ammonia-N increased from 0 to 29 mg/L, while that of nitrite-N increased to 1.5 mg/L in the first 30 min, then decreased to 0.9 mg/L after 90 min. With the addition of 0.5 g/L NaCl (Fig. 6 (b)), the concentration of nitrate decreased from 50 to 12.1 mg/L. The accumulation of ammonia-N

was lower than in the NaCl-free case, reaching only19.1 mg/L after 90 min. The concentration of nitrite-N increased to 0.4 mg/L after the first 30 min, then decreased to 0.25 mg/L after 90 min. Thus, it was clear that the addition of NaCl effectively removed ammonia-N and nitrite-N by-products.

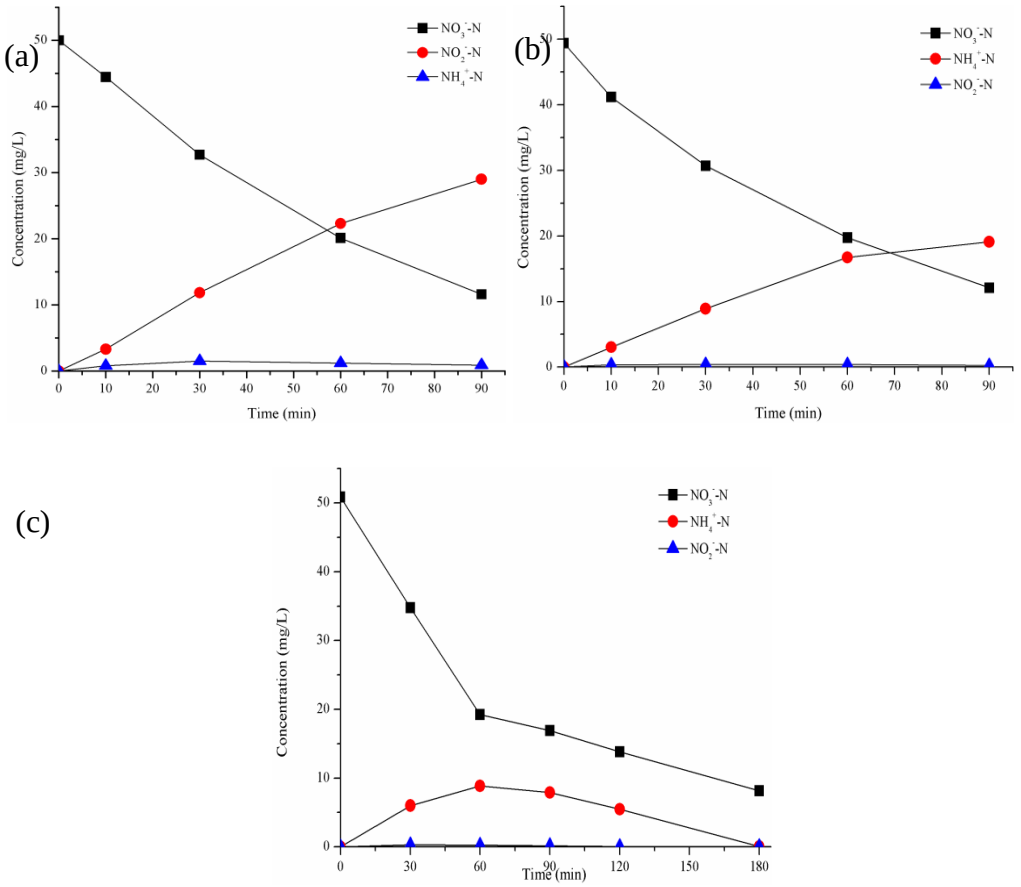

Figure 6. Electroreduction of nitrate in time of different concentrations of NaCl (a) no NaCl, (b) 0.5 g/L NaCl, (c) 1.0 g/L NaCl, I = 50 mA/cm^2, 0.50 g/L Na_2SO_4

During electrolysis, the oxidizing hypochlorite ion is formed in the presence of chloride ions; thus, the main electrochemical reactions were as follows [40]:

$$2Cl^- \rightarrow Cl_2 + 2e^- \quad (12)$$

$$Cl_2 + H_2O \rightarrow HClO + H^+ + Cl^- \quad (13)$$

$$HClO \rightarrow ClO^- + H^+ \quad (14)$$

The hypochlorous acid formed during electrolysis oxidizes ammonia and nitrite into nitrogen gas and nitrate [41]:

$$NH_4^+ + HClO \rightarrow N_2 + H_2O + H^+ + Cl^- \quad (15)$$

$$NO_2^- + HClO \rightarrow NO_3^- + H_2O + Cl^- \quad (16)$$

As is shown, the concentrations of ammonia and nitrite decreased as the NaCl addition increased. In the presence of 1.0 g/L NaCl (Fig.6 (c)), the concentration of nitrate decreased from 50 to 8.15 mg/L in 180 min. That of ammonia-N increased from 0 to 8.85 mg/L in the first 60 min, then decreased to 0.055 mg/L after 180 min, while only a negligible amount of nitrite-N was detected

throughout the entire 180 min of electrolysis. The nitrate reduction efficiency without NaCl addition was higher than that with NaCl addition, mainly because nitrate reduction was retarded in the presence of chloride [42]. In this study, the addition of 1.0 g/L NaCl produced enough hypochlorous acid to completely oxidize ammonia and nitrite. The optimal NaCl addition was thus 1.0 g/L in the present study.

4. CONCLUSIONS

A novel Ti-based nano-electrode was fabricated to improve the efficiency of electroreduction of nitrate. The results of SEM-EDS and XPS demonstrated that the surface of the Ti-based nano-electrode was covered with a large number of nanoparticles, as well as relatively homogenous tubular structure, and the main component of the Ti-based nano-electrode was TiO_2. The results of CV suggested that the Ti-based nano-electrode was capable of enhanced electrochemical activity. Using Ti-based nano-electhrode as a cathode, with a Ti/Pt anode, the electrochemical removal of nitrate proceeded efficiently. The initial nitrate concentration and the temperature exerted slight effects on the nitrate removal. The addition of NaCl was found to positively affect the removal of ammonia and other by-products, thereby achieving the goal of clean, safe removal of nitrate.

ACKNOWLEDGEMENTS
The authors thank the National Natural Science Foundation of China (No.51408335) for the financial support of this work.

References

1. N.F. Gray, *Drinking Water Quality: Problems and Solutions*, John Wiley and Sons, Inc., Chichester (1994).
2. D.Majumdar, N.Gupta, *Indian J. Environ. Health*, 42(2000) 28.
3. Y. Fernandez-Nava, E. Maranon, J. Soons, L. Castrillon, *Bioresour. Technol.*, 17(2008)7976.
4. S.K. Gupta, R.C. Gupta, A.B. Gupta, A.K. Seth, J.K. Bassin, *Environ. Health Perspect.*, 108(2000) 363.
5. P. Dold, I. Takacs, Y. Mokhayeri, A. Nichols, J. Hinojosa, R. Riffat, C. Bott, W .Bailey, S. Murthy, *Water Environ., Res*., 80(2008)417.
6. WHO, *Rolling revision of the WHO guidelines for drinking-water quality,nitrates and nitrites in drinking water*. World Health Organization. Geneva,Switzerland (2004).
7. Environmental Protection Agency US *Drinking water regulations, health advisories*. Office of Water, Washington, DC (1995).
8. S. Ghafari, M. Hasan, M.K. Aroua, *Bioresour. Technol.*, 99 (2008) 3965.
9. J. Park, H. Byun, W. Choi, W. Kang, Chemosphere, 70 (2008) 1429.
10. P.A. *Terry, Environ Eng. Sci.*, 26 (2009) 691.
11. G. Zhao, Y. Zhang, Y. Lei, B. Lv, J. Gao, D. Li, Y. Zhang, *Environ. Sci. Technol.*, 44(2010)1754.
12. M. Li, C. Feng, Z. Zhang, N. Sugiura, *Electrochim. Acta*, 54(2009) 4600.
13. I. Katsounaros, M. Dortsiou, G. Kyriacou, *J. Hazard. Mater.*, 171(2009)323.
14. H.L. Li, J.Q. Chambers, D.T. Hobbs, *J. Appl. Electrochem.*, 18(1988)454.

15. J. Souza-Garcia, E.A. Ticianelli, V. Climent, J.M. Feliu, *Electrochim. Acta*., 54 (2009)2094.
16. D. Reyter, D. Bélanger, L. Roue, *Electrochim. Acta*, 53 (2008) 5977.
17. A. Olad, F. Farshi, J. Ettehadi, *Water Environ. Res*., 84(2012)144.
18. D. Reyter, D. Bélanger, L. Roué, *J. Phys. Chem. C*., 113 (2009)290.
19. G.E. Badea, *Electrochim. Acta*, 54 (2009) 996.
20. O. Brylev, M. Sarrazin, L. Roué, D. Bélanger, *Electrochim. Acta*, 52 (2007) 6237.
21. Y. L. Su, Y. T. Xiao, Y. X. Du, S. Fu, *Chem. Phys*., 20(2010) 2136.
22. N.K. Allam, K. Shankar, C.A. Grimes, *J. Mater. Chem*., 18(2008)2341.
23. A. Fujishima, K. Honda, *Nature*, 238(1972) 37.
24. Y.Y. Kuo, T.H. Li, J.N. Yao, C.Y. Lin, C.H. Chen, *Electrochim. Acta*, 78(2012)236.
25. Y. Xie, G. Ali, S.H. Yoo, S.O. Cho, *ACS Appl. Mater. Interfaces*, 2(2010) 2910.
26. R. Carbone, I. Marangi, A. Zanardi, L. Giorgetti, E. Chierici, G. Berlanda, A. Podestà, F. Fiorentini, G. Bongiorno, P. Piseri, P. Pelicci, P. Milani, *Biomaterials*, 27 (2006) 3221.
27. J.H. Park, S. Kim, A.J. Bard, *Nano Lett*., 6(2006)24.
28. L.L. Wang, M. Li, C.P. Feng, W.W. Hu, G.Y. Ding, N. Chen, X. Liu, *J. Electroanal. Chem.*, 773 (2016) 13.
29. F. Liu, M. Li, H. Wang, X.H. Lei, X. Liu, L.L. Wang. *Int. J. Electrochem. Sci.*, 11(2016)8308.
30. F. Liu, M. Li, H. Wang, X.H. Lei, L.L. Wang, X. Liu. *J. Electrochem. Soc.*, 163(2016)E421.
31. I. Paramasivam, H. Jha, N. Liu, P. Schmuki, *Small*, 8(2012)3073.
32. APHA, AWWA, WPCF, *American Public Health Association*, Washington, DC, USA (1998).
33. D. B. Hamal, K. J. Klabunde, *J. Phys. Chem. C*, 115(2011) 17359.
34. G. B. Soares, B. Bravin, C. M. P. Vaz, C. Ribeiro, *Appl. Catal. B-Environ.*, 106(2011) 287.
35. G. Li, Z. Q. Liu, Z. Zhang, X. Yan, *Chinese J. Catal.*, 30(2009) 37.
36. F. Zhang, S. Chen, Y. Yin, C. Lin, C. Xue, *J. Alloys Compd.*, 490 (2010) 247.
37. J. Bai, B. Zhou, L. Li, Y. Liu, Q. Zheng, J. Shao, X. Zhu, W. Cai, J. Liao, L. *Zou, J Mater Sci.*, 43 (2008) 1880.
38. M. Li, C. Feng, Z. Zhang, Z. Shen, N. Sugiura, *Electrochem. Commun.*, 11 (2009)1853.
39. H. Cheng, K. Scott, P.A. Christensen, *J. Appl. Electrochem.*, 35(2005)551.
40. L. Li, Y. Liu, *J. Haz. Mater.*, 161(2009) 1010.
41. M. Li, C. P. Feng, Z. Y. Zhang, *J. Haz. Mater.*, 171(2009) 724.
42. I. Katsounaros, G. Kyriacou, *Electrochim. Acta.*, 52(2007) 6412.